[19] W. S. Metcalf, "Cascading 4-port networks," *Microwave J.*, vol. 12, pp. 77–82, Sept. 1969.
[20] R. L. Ernst, R. L. Camisa, and A. Presser, "Graceful degradation properties of matched *n*-port power amplifier combiners," in *MTT-S Int. Microwave Symp. Dig.*, pp. 174–177, June 1977.
[21] A. A. M. Saleh, "Improving the graceful-degradation performance of combined power amplifiers," *IEEE Trans. Microwave Theory Tech.*, vol. MTT-28, pp. 1068–1070, 1980.

Suspended Slot Line Using Double Layer Dielectric

RAINEE SIMONS, MEMBER, IEEE

Abstract—**This paper presents a rigorous analysis of a) slot line on a double layer dielectric substrate, and b) slot line sandwiched between two dielectric substrates. The structure is assumed to be suspended inside a conducting enclosure of arbitrary dimensions. The dielectric substrates are assumed to be isotropic and homogeneous and are of arbitrary thickness and relative permittivity. The conducting enclosure and the zero thickness metallization on the substrate, are assumed to have infinite conductivity. The effect of shielding on the dispersion, characteristic impedance, and the effective dielectric constant are illustrated. These results should find application in the design and fabrication of MIC components and subsystems.**

I. Introduction

Slot line on a dielectric substrate is a very useful transmission line for microwave and millimeter-wave integrated circuit applications [1]–[3]. Recently, two new slot line structures have been proposed; namely, slot line on a double layer dielectric substrate [4] and the sandwich slot line [5], [6]. These structures are a modification of the regular slot line originally proposed by Cohn [7]. In regular slot line a narrow slot is etched out in the conductive coating on one side of a dielectric substrate; the other side of the substrate being bare.

In the slot line on a double layer dielectric substrate, shown in Fig. 1, the regular slot line is modified by introducing an additional dielectric layer (region 2) between the conductive coating and the substrate (region 3). By choosing the dielectric constant of region 3 larger than that of region 2, one can divert the electromagnetic energy flow away from the conductive coating [4]. Hence in this structure the loss due to the conductor can be reduced, and, at the same time, the conductive coating provides a heat sink and is convenient for dc biasing in solid-state device application [4]. The double layer slot line when compared with the regular slot line with identical slot width has a larger characteristic impedance. The sandwich slot line, shown in Fig. 2, with top dielectric layer of low permittivity is also useful at millimeter-wave frequencies. However, it has a slightly higher value of effective dielectric constant when compared with the double layer slot line with same permittivities. The sandwiched slot line when compared with the regular slot line with identical relative permittivities offers the advantages of shorter wavelength and greater confinement of the electromagnetic fields within the dielectric.

The slot line on a double layer dielectric substrate in the unshielded form was first analyzed by Samardzija and Itoh [4].

Manuscript received March 4, 1981; revised June 3, 1981.
The author is with the Centre for Applied Research in Electronics, Indian Institute of Technology Delhi, Hauz Khas, New Delhi 11016, India.

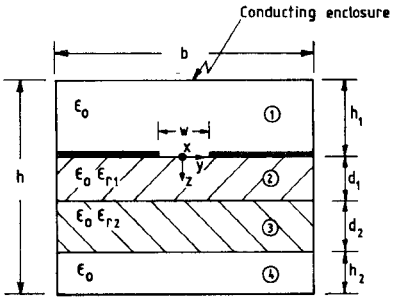

Fig. 1. Cross-sectional view of the slot line on a suspended double layer dielectric substrate.

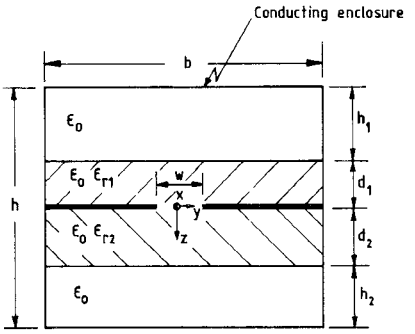

Fig. 2. Cross-sectional view of the suspended sandwich slot line.

However, only to the extent that the dispersion characteristic were computed and illustrated. The slot line sandwiched between two dielectric substrates was first analyzed by Cohn [5]. Based on Cohn's analysis, Mariani and Agrios [6] computed the dispersion and characteristic impedance for a wide variety of substrate materials. However, their data are valid only for the unshielded structure. Invariably a practical system is shielded from the environment in order to protect it from RF interference. Hence an analysis which takes into account the presence of a shielding enclosure and allow a study of its influence is felt.

The paper analyzes, firstly, the slot line on a double layer dielectric substrate suspended inside a conducting enclosure of arbitrary dimensions, secondly, slot line sandwiched between two dielectric substrates suspended inside a conducting enclosure of arbitrary dimensions. The dielectric substrates are assumed to be isotropic and homogeneous and are of arbitrary thickness and relative permittivity. The conducting enclosure and the zero thickness metallization on the substrate, are assumed to have infinite conductivity.

The above structures are analyzed using Cohn's technique [7], which is extended here to take into account more than one dielectric substrate on a given side of the slot and also the effect of a shielding enclosure. For the modeling of the open structure the shielding enclosure is allowed to expand to infinity without causing numerical problems or increasing computing time.

II. Analysis

A. Slot Line on a Double Layer Dielectric Substrate

The schematic diagram of the structure to be analyzed is shown in Fig. 1. In this structure slot waves of equal amplitude traveling in the $+x$ and $-x$ directions are taken into consideration. As a consequence there exist, along the slot line, transverse planes separated by $\lambda'/2$, where λ' is the wavelength in the slot line. At

0018-9480/81/1000-1102$00.75 ©1981 IEEE

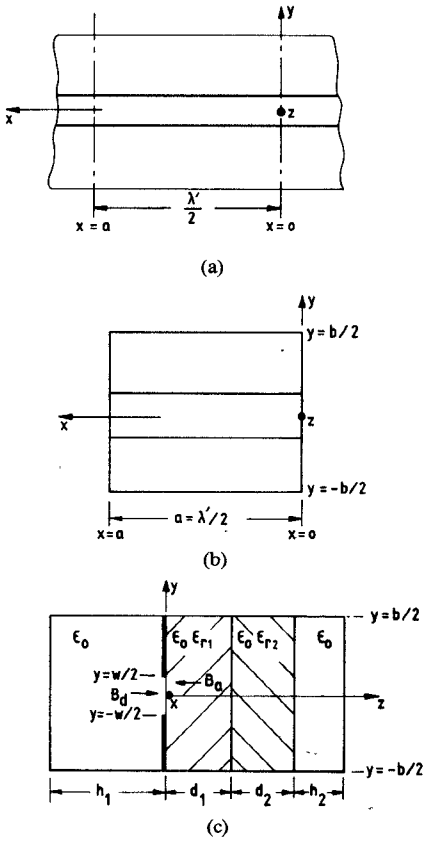

Fig. 3. (a) Insertion of transverse conducting walls at $x=0$ and $x=a$. (b) Elimination of the semi-infinite regions $x<0$ and $x>a$. (c) Waveguide model containing capacitive iris and dielectric slab.

these planes the transverse electric (TE) field and the normal magnetic field get cancelled and become zero. Two such planes occur at $x=0$ and $x=\lambda'/2=a$, and this is shown in Fig. 3(a). Furthermore, electric walls can be inserted at these points without disturbing the field components between them and the semi-infinite regions $x<0$ and $x>a$ can be eliminated, as shown in Fig. 3(b). Thus the region that is separated from the original structure can be considered as a rectangular waveguide with a symmetric capacative iris backed by a dielectric substrate, as in Fig. 3(c). The complete set of modes satisfying the boundary conditions of this structure are $TE_{1,2n}$ for n an integer ≥ 0 and $TM_{1,2n}$ for n an integer ≥ 1.

Since the wavelength in the slot line is less than the free-space wavelength λ, it follows that a is less than $\lambda/2$. Therefore, the TE_{10} and all higher order modes are cutoff or nonpropagating in the air regions. In the dielectric region the TE_{10} mode is propagating, and the first few higher modes may propagate or all the higher modes may be cutoff depending upon the height of the waveguide b. When transverse resonance occurs the sum of the susceptances at the plane of the iris is zero. This sum includes the susceptance of the TE_{10} mode looking in the $-z$ and $+z$ directions, and the capacitive iris susceptance representing the $TE_{1,2n}(n>0)$ and $TM_{1,2n}(n>0)$ modes on the $-z$ and $+z$ sides of the iris. Let B_d be the susceptance at the plane of the iris ($z=0$), as seen to the right into the dielectric substrate, and B_a be the susceptance at the plane of the iris ($z=0$), as seen to the left into the air region. Then the sum of the susceptances B_t at the plane of the iris ($z=0$) is B_d+B_a. To obtain a solution for $B_t=0$ an independent variable $p=\lambda/2a$ is defined. At the transverse resonance frequency $a=\lambda'/2$ and $p=\lambda/\lambda'$ for $B_t=0$. The wavelength and frequency for this solution are $\lambda=2a(\lambda/\lambda')$ and $f=c/\lambda$. An expression for B_d will be derived first and then modified to yield B_a.

The total E_y and H_x fields at the $z=0$ plane and $x=a/2$ are functions of y as follows:

$$E_y = R_0 + \sum_{n=1,2,\cdots}^{\infty} R_n \cos\frac{2\pi n y}{b} \tag{1}$$

$$H_x = -y_{i0}R_0 - \sum_{n=1,2,\cdots}^{\infty} y_{in}R_n \cos\frac{2\pi n y}{b} \tag{2}$$

where R_0 and R_n are constants, and input wave admittances y_{i0} and y_{in} are defined by

$$y_{i0} = -\left(\frac{H_x}{E_y}\right)_{TE_{10}} \tag{3}$$

$$y_{in} = -\left(\frac{(H_x)_{TE_{1,2n}}+(H_x)_{TM_{1,2n}}}{(E_y)_{TE_{1,2n}}+(E_y)_{TM_{1,2n}}}\right). \tag{4}$$

Next, it is assumed that in the slot of width w at the $z=0$ plane, only the TE_{10} mode is present under this assumption E_y and H_x are constants as follows:

$$E_y = \begin{cases} C_0, & \text{for } |y|\leq w/2 \\ 0, & \text{for } w/2<|y|\leq b/2 \end{cases} \tag{5}$$

$$H_x = -C_0 y_i', \quad \text{for } |y|\leq w/2 \tag{6}$$

where y_i' is input wave admittance as seen to the right at the $z=0$ plane. Equation (1) has the form of a Fourier series. Let this series equal E_y as defined in (5). Then R_0 and R_n are determined

as follows:

$$R_0 = C_0\delta \qquad R_n = 2C_0\delta\frac{\sin\pi n\delta}{\pi n\delta} \tag{7}$$

where $\delta = w/b$. Next, set the right-hand sides of (2) and (6) equal, and integrate with respect to y over the slot of width w. Further, substitute for R_0 and R_n from (7) and replace the wave admittances by guide admittance defined on the TE_{10}-mode voltage power basis in the complete waveguide cross section. Then the input wave admittance as seen to the right at the $z=0$ plane is

$$Y_t = jB_d = Y_{t0} + 2\sum_{n=1,2,\cdots}^{\infty} Y_{tn}\left(\frac{\sin\pi n\delta}{\pi n\delta}\right)^2 \tag{8}$$

where Y_{t0} is the admittance seen by a TE_{10} mode wave directed into dielectric filled waveguide region of length d_1+d_2 terminated by an air-filled region of length h_2. Y_{t0} can be easily shown to be equal to

$$Y_{t0} = \frac{au_1}{2b}\tan\left[\frac{\pi u_1 d_1}{ap} + \tan^{-1}\cdot\left\{\frac{u_2}{u_1}\tan\left(\frac{\pi u_2 d_2}{ap} - \tan^{-1}\frac{v}{u_2}\coth\gamma h_2\right)\right\}\right] \tag{9}$$

where

$$\begin{aligned} u_1 &= (\epsilon_{r1} - p^2)^{1/2} \\ u_2 &= (\epsilon_{r2} - p^2)^{1/2} \\ v &= (p^2 - 1)^{1/2} \\ \gamma &= vk. \end{aligned} \tag{10}$$

γ is the TE_{10} mode propagation constant in the air regions and $k = 2\pi/\lambda$. Y_{tn} is the admittance seen by the higher order TE and TM modes directed into the dielectric region. For each n, the corresponding TE and TM amplitudes must be so chosen so that E_x exactly cancells at $z=0$. In this way the total E_x field will be zero at $z=0$, as is required by the boundary condition in that transverse plane. When this condition is imposed it can easily be shown that

$$Y_{tn} = \frac{Y_{t\,TM_n} + Y_{t\,TE_n}(b/2an)^2}{1+(b/2an)^2} \tag{11}$$

and the input admittances $Y_{t\,TM_n}$ and $Y_{t\,TE_n}$ for each n are

$$Y_{t\,TM_n} = \frac{j\epsilon_{r1}}{4pnF_{n1}\eta}\tanh\left[\frac{2\pi nF_{n1}d_1}{b} + \tanh^{-1}\frac{\epsilon_{r2}}{\epsilon_{r1}}\frac{F_{n1}}{F_{n2}}\tanh\left\{\frac{2\pi nF_{n2}d_2}{b} + \tanh^{-1}\frac{1}{\epsilon_{r2}}\frac{F_{n2}}{F_n}\coth\left(\frac{2\pi nF_n h_2}{b}\right)\right\}\right] \tag{12}$$

$$Y_{t\,TE_n} = \frac{a\gamma_{n1}}{j2b\eta k}\coth\left[\frac{2\pi nF_{n1}d_1}{b} + \coth^{-1}\frac{F_{n2}}{F_{n1}}\coth\left\{\frac{2\pi nF_{n2}d_2}{b} + \coth^{-1}\frac{F_n}{F_{n2}}\coth\left(\frac{2\pi nF_n h_2}{b}\right)\right\}\right] \tag{13}$$

where

$$\begin{aligned} \eta &= \sqrt{\mu_0/\epsilon_0} = 376.7\,\Omega \\ F_{n1} &= \sqrt{1-\left(\frac{bu_1}{2anp}\right)^2} \\ F_{n2} &= \sqrt{1-\left(\frac{bu_2}{2anp}\right)^2} \\ F_n &= \sqrt{1+\left(\frac{bv}{2anp}\right)^2}. \end{aligned} \tag{14}$$

Equations (8)–(14) yield the susceptance B_d looking to the right at the plane $z=0$. However, the rate of convergence of this series is very slow and can be improved as explained in [7]. With the modification, (8), the susceptance looking into the dielectric region, is

$$\eta B_d = \frac{au_1}{2b}\tan\left[\frac{\pi u_1 d_1}{ap} + \tan^{-1}\cdot\left\{\frac{u_2}{u_1}\tan\left(\frac{\pi u_2 d_2}{ap} - \tan^{-1}\frac{v}{u_2}\coth vkh_2\right)\right\}\right] + \frac{u_1^2}{2p}\ln\left(\frac{2}{\pi\delta}\right) + \frac{1}{2p}\sum_{n=1,2,\cdots}^{\infty}\cdot\left[\frac{\epsilon_{r1}\tanh r_n - p^2F_{n1}^2\coth q_n}{\left[1+\left(\frac{b}{2an}\right)^2\right]F_{n1}} - u_1^2\right]\cdot\frac{\sin^2\pi n\delta}{n(\pi n\delta)^2} \tag{15}$$

The susceptance B_a looking to the left from the plane of the iris is obtained from (15) by letting $\epsilon_{r1}=\epsilon_{r1}=1$ or $d_1=d_2=0$, and $h_1=h_2$. With these substitutions the following result is obtained:

$$\eta B_a = -\frac{av}{2b}\coth vkh_1 - \frac{v^2}{2p}\ln\left(\frac{2}{\pi\delta}\right) + \frac{1}{2p}\sum_{n=1,2,\cdots}^{\infty}\left[v^2\left\{1-\frac{\coth(2\pi nF_n h_1/b)}{F_n}\right\}\right]\cdot\frac{\sin^2(n\pi\delta)}{n(n\pi\delta)^2} \tag{16}$$

when (15) and (16) are added, the sum of the susceptances B_t at the plane of the iris is obtained

$$\eta B_t = \frac{a}{2b}\left\{-v\coth(vkh_1) + u_1\tan\left[\frac{\pi d_1 u_1}{ap} + \tan^{-1}\cdot\left\{\frac{u_2}{u_1}\tan\left(\frac{\pi d_2 u_2}{ap} - \tan^{-1}\frac{v}{u_2}\coth vkh_2\right)\right\}\right]\right\} + \frac{1}{p}\left\{\left(\frac{\epsilon_{r1}+1}{2} - p^2\right)\ln\frac{2}{\pi\delta} + \frac{1}{2}\sum_{n=1,2,\cdots}^{\infty}\left[v^2\left(1-\frac{\coth(2\pi nF_n h_1/b)}{F_n}\right) + M_n\right]\cdot\frac{\sin^2(\pi n\delta)}{n(\pi n\delta)^2}\right\}. \tag{17}$$

For F_{n1} and F_{n2} real, M_n is

$$M_n = \frac{\epsilon_{r1}\tanh r_n - p^2 F_{n1}^2 \coth q_n}{\left\{1+(b/2an)^2\right\} F_{n1}} - u_1^2 \tag{18}$$

where

$$r_n = \frac{2\pi n F_{n1} d_1}{b} + \tanh^{-1} \cdot \left[\frac{\epsilon_{r2}}{\epsilon_{r1}} \frac{F_{n1}}{F_{n2}} \tanh \left\{ \frac{2\pi n F_{n2} d_2}{b} + \tanh^{-1} \left(\frac{1}{\epsilon_{r2}} \frac{F_{n2}}{F_n} \cdot \coth \left(\frac{2\pi n F_n h_2}{b} \right) \right) \right\} \right] \tag{19}$$

$$q_n = \frac{2\pi n F_{n1} d_1}{b} + \coth^{-1} \cdot \left[\frac{F_{n2}}{F_{n1}} \coth \left\{ \frac{2\pi n F_{n2} d_2}{b} + \coth^{-1} \left(\frac{F_n}{F_{n2}} \cdot \coth \left(\frac{2\pi n F_n h_2}{b} \right) \right) \right\} \right]. \tag{20}$$

B. Slot Line Sandwiched Between Two Dielectric Substrates

The schematic diagram of the structure is shown in Fig. 2. The expression for the total susceptance B_t at the plane of the iris is obtained using Cohn's [7] technique and is as follows:

$$\eta B_t = \frac{a}{2b} \left\{ u_1 \tan \left[\frac{\pi d_1 u_1}{ap} - \tan^{-1} \left(\frac{v}{u_1} \coth vkh_1 \right) \right] + u_2 \tan \left[\frac{\pi d_2 u_2}{ap} - \tan^{-1} \cdot \left(\frac{v}{u_2} \coth vkh_2 \right) \right] \right\} + \frac{1}{p} \left\{ \left(\frac{\epsilon_{r1}+\epsilon_{r2}}{2} - p^2 \right) \cdot \ln \frac{2}{\pi\delta} + \frac{1}{2} \sum_{n=1,2,\cdots}^{\infty} (M_{n1}+M_{n2}) \cdot \frac{\sin^2(n\pi\delta)}{n(n\pi\delta)^2} \right\}. \tag{21}$$

For F_{ni} real, $i=1$ or 2,

$$M_{ni} = \frac{\epsilon_{ri}\tanh r_{ni} - p^2 F_{ni}^2 \coth q_{ni}}{\left[1+(b/2an)^2\right] F_{ni}} - u_i^2 \tag{22}$$

where

$$r_{ni} = \frac{2\pi n d_i F_{ni}}{b} + \tanh^{-1} \cdot \left[\left(\frac{F_{ni}}{F_n \epsilon_{ri}} \right) \coth (2\pi n F_n h_i / b) \right] \tag{23}$$

and

$$q_{ni} = \frac{2\pi n d_i F_{ni}}{b} + \coth^{-1} \cdot \left[\left(\frac{F_{ni}}{F_n} \right) \coth (2\pi n F_n h_i / b) \right]. \tag{24}$$

III. Guide Wavelength and Characteristic Impedance

The values of ϵ_r, d, w, b, h, and $a=\lambda'/2$ are substituted into (17) and (21) and solved for the value of p at which $\eta B_t = 0$. This p is equal to λ/λ'.

The ratio of phase velocity to group velocity is defined as follows [7]:

$$\frac{v}{v_g} = 1 + \frac{f}{\lambda/\lambda'} \frac{\Delta(\lambda/\lambda')}{\Delta f} \tag{25}$$

where $\Delta(\lambda/\lambda')$ and Δf are computed from two separate solutions of $\eta B_t = 0$ for fixed values of ϵ_r, d, w, b, h, and for two slightly different values of $a=\lambda'/2$ incremented plus and minus from the desired a. The frequency f is assumed to lie midway in the Δf interval.

The slot-wave characteristic impedance Z_0 is defined as follows [7]:

$$Z_0 = 376.7 \frac{v}{v_g} \frac{\pi}{p} \frac{\Delta p}{-\Delta(\eta B_t)} \Omega. \tag{26}$$

$\Delta(\eta B_t)$ is computed from (17) with ϵ_r, d, w, b, h, and a held fixed, and with p incremented slightly plus and minus from the value $p=\lambda/\lambda'$ at $\eta B_t = 0$.

IV. Numerical Results

The computed relative wavelength λ'/λ and characteristic impedance Z_0 of both the structures are illustrated in Figs. 4 and 5, respectively. Figs. 4(a) and 5(a) illustrate the variation of the relative wavelength ratio λ'/λ, and characteristic impedance Z_0, as a function of the normalized substrate thickness with the normalized slot width as a parameter. The height of the conducting enclosure is held fixed.

Figs. 4(b) and 5(b) illustrate the variation of λ'/λ, and Z_0 as a function of the normalized substrate thickness with normalized height of the conducting enclosure as a parameter. The normalized slot width is held fixed. It is observed that as the height of the conducting enclosure is gradually reduced, starting from a large value, the slot-mode slowly cuts off.

The variation of the effective dielectric constant ϵ_{eff} of both the structures as a function of the normalized substrate thickness with the height of the conducting enclosure as a parameter, are illustrated in Figs. 6 and 7, respectively. Close agreement is

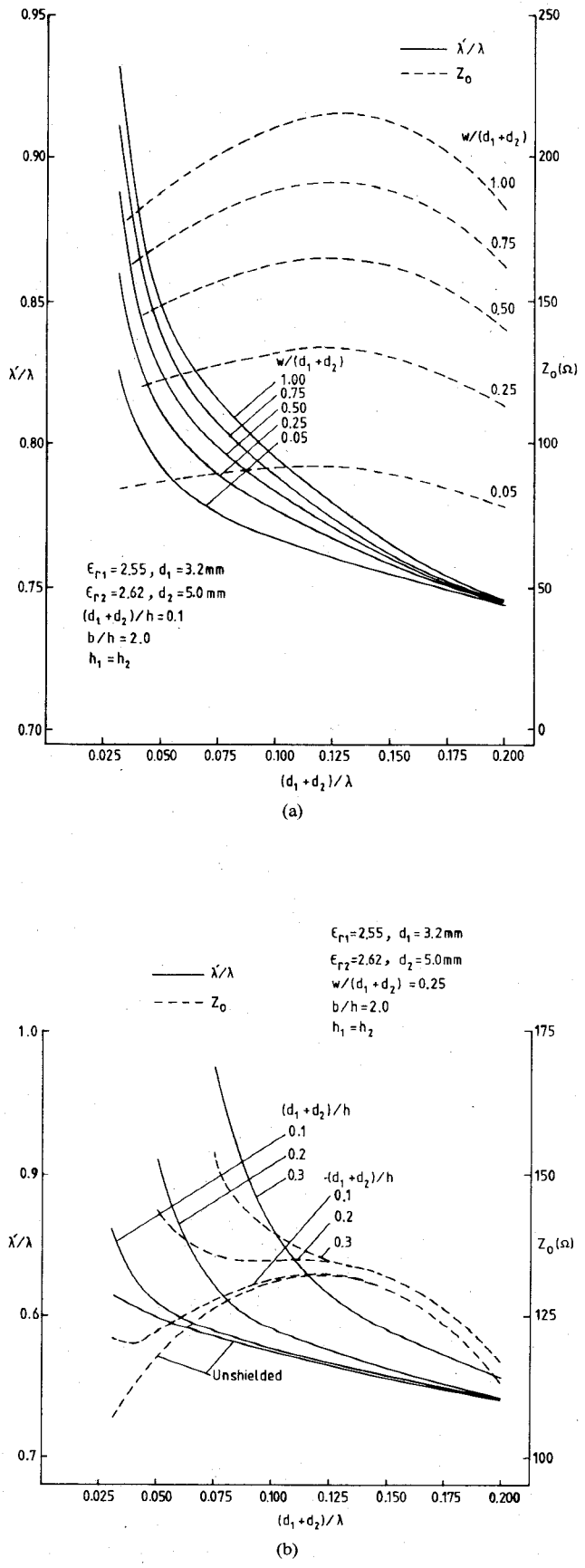

Fig. 4. (a) The variation of relative wavelength λ'/λ and characteristic impedance Z_0 with $(d_1+d_2)/\lambda$, when the height of the conducting enclosure remains fixed. (b) The effect of shielding on the relative wavelength λ'/λ and characteristic impedance Z_0.

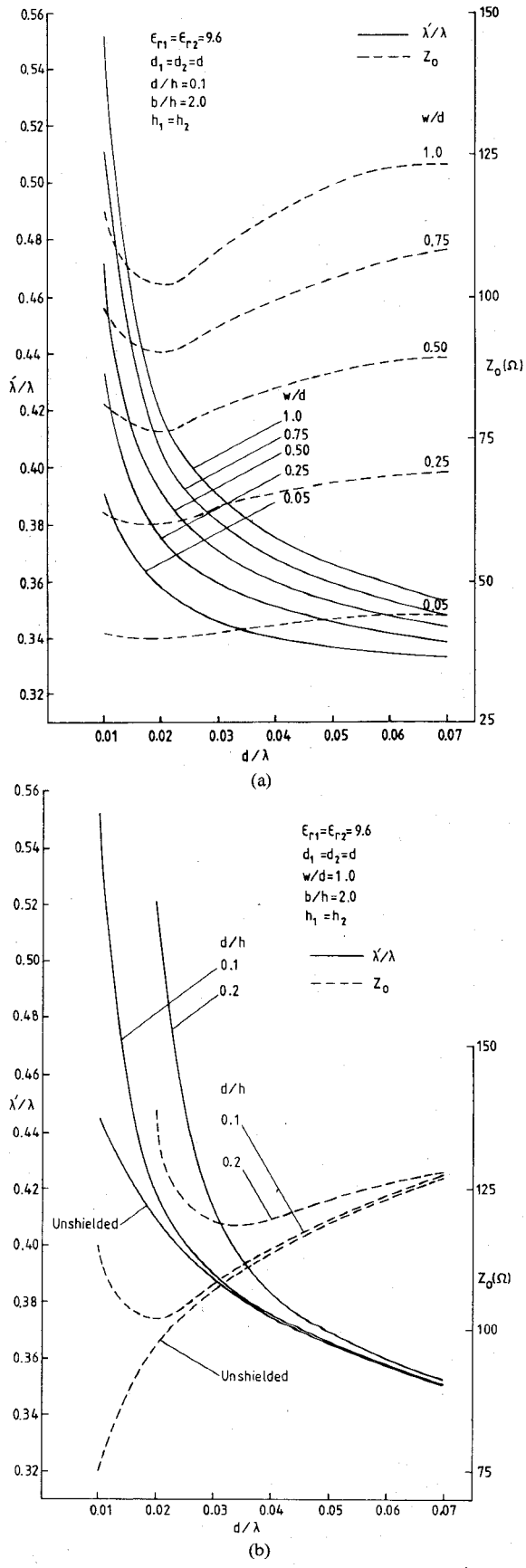

Fig. 5. (a) The variation of relative wavelength λ'/λ and characteristic impedance Z_0 with d/λ, when the height of the conducting enclosure remains fixed. (b) The effect of shielding on the relative wavelength λ'/λ, and characteristic impedance Z_0.

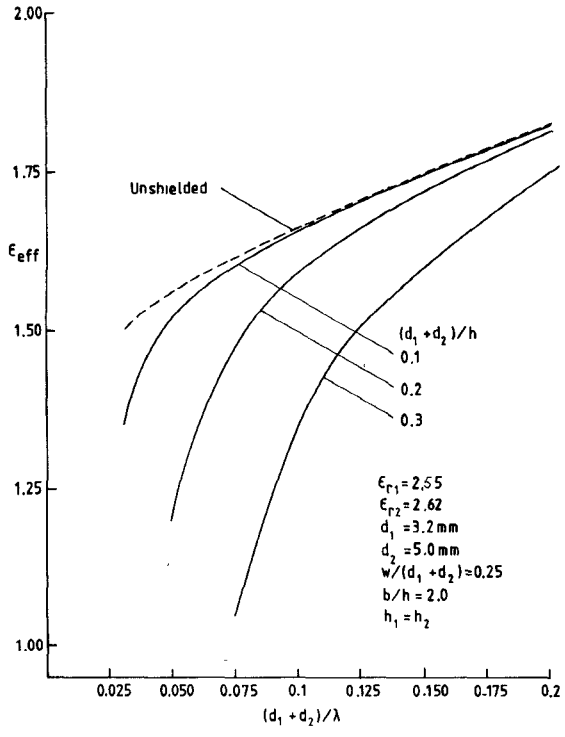

Fig. 6. The effect of shielding on the effective dielectric constant ϵ_{eff}.

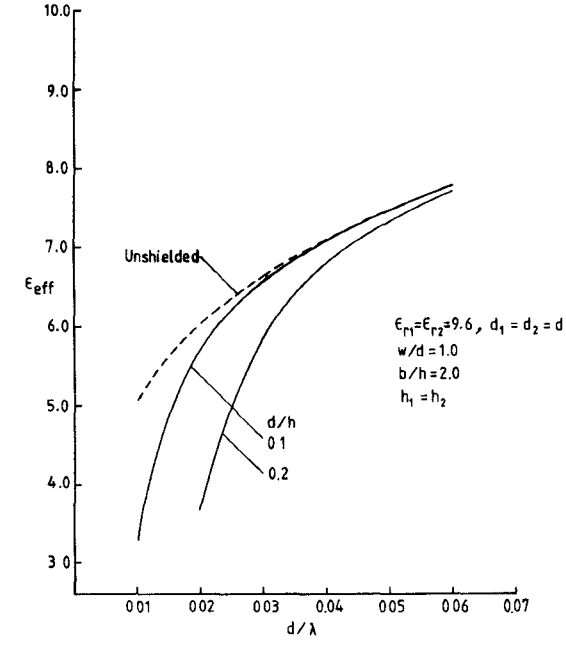

Fig. 7. The effect of shielding on the effective dielectric constant ϵ_{eff}.

observed between the unshielded case and for the case when the normalized height is equal to 0.1. This is expected since the effect of the conducting enclosure diminishes with increasing frequency.

V. Conclusion

Briefly, the paper presents an analysis of shielded slot line a) on a double layer dielectric substrate, and b) sandwiched between two dielectric substrates. The computed results illustrate the dispersion and characteristic impedance of the two structures. The effect of shielding on the dispersion, characteristic impedance and effective dielectric constant are also illustrated. These results should find extensive application in the design and fabrication of MIC components.

References

[1] B. Schiek, "Hybrid Branchline couplers—A useful new class of directional couplers," *IEEE Trans. Microwave Theory Tech.*, vol. MTT-22, pp. 864–869, Oct. 1974.
[2] M. E. Davis, "Integrated diode phase-shifter elements for an *X*-band phased-array antenna," *IEEE Trans. Microwave Theory Tech.*, vol. MTT-23, pp. 1080–1084, Dec. 1975.
[3] L. E. Dickens and D. W. Maki, "An integrated-circuit balanced mixer, image and sum enchaned," *IEEE Trans Microwave Theory Tech.*, vol. MTT-23, pp. 276–281, Mar. 1975.
[4] N. Samardzija and T Itoh, "Double-layered slot-line for millimeter-wave integrated circuits," *IEEE Trans Microwave Theory Tech.*, vol. MTT-24, pp. 827–831, Nov. 1976.
[5] S. B. Cohn, "Sandwich slot-line," *IEEE Trans. Microwave Theory Tech.*, vol. MTT-19, pp. 773–774, Sept. 1971.
[6] E. A. Mariani and J. P. Agrios, "Slot-line filters and couplers," *IEEE Trans. Microwave Theory Tech.*, vol. MTT-18, pp. 1089–1095, Dec. 1970.
[7] S B. Cohn, "Slot-line on a dielectric substrate," *IEEE Trans. Microwave Theory Tech.*, vol. MTT-17, pp. 768–778, Oct. 1969.
[8] I. S. Gradshteyn and I. M. Ryzhik, *Table of Integrals, Series, and Products*. New York and London: Academic, 1965, (ch. 2, art. 20.1 (17)), p. 54, and (Ch. 3–4, art. 3.753 (2)), p. 419.
[9] S. B. Cohn, "Slot-line on a dielectric substrate," *IEEE Trans. Microwave Theory Tech.*, vol. MTT-17, pp. 768–778, Oct. 1969.
[10] R. E. Collin, *Field Theory of Guided Waves*. New York: McGraw-Hill, 1960. (Use $\Sigma_{1,2,3}\ (\exp jnx)/n^3$ on p. 579.)
[11] N. Marcuvitz, Waveguide Handbook, M.I.T. Rad. Lab. Ser., vol. 10, New York: McGraw-Hill, 1951, pp. 218–219.
[12] T Itoh and R. Mittra, "Dispersion characteristic of slot Lines," *Electron. Lett.*, vol. 7, pp. 364–365, July 1971.
[13] J. B. Knorr and K D. Duchler, "Analysis of coupled slots and coplanar strips on dielectric substrate," *IEEE Trans. Microwave Theory Tech.*, vol. MTT-23, pp. 541–548, July 1975. (see Fig 2.)
[14] E. A Mariani, C. P. Heinzman, J. P. Agrios, and S. B. Cohn, "Slot line characteristics," *IEEE Trans. Microwave Theory Tech.*, vol. MTT-17, pp. 1091–1096, Dec. 1969.

Open-End Discontinuity in Shielded Microstrip Circuits

S.S. BEDAIR AND M. I. SOBHY, MEMBER, IEEE

***Abstract*—This short paper gives closed-form expressions for the open-end discontinuity in shielded microstrip circuits. These expressions consider the effect of dispersion at very high frequencies and are based on the results obtained earlier for the stripline configuration. The test of validity of these expressions is performed by comparison with the limit case of the unshielded microstrip.**

I. Introduction

A set of closed-form expressions was derived [1] for the computer-aided design of shielded microstrip circuits with zero strip thickness. In this configuration, the circuit performance can be controlled by adjusting the shield heights ratio. These expressions were for the calculation of the capacitances, characteristic imped-

Manuscript received January 7, 1981; revised April 30, 1981.
The authors are with the Electronic Laboratories, the University of Kent at Canterbury, Canterbury, Kent, CT2 7NT, UK.

0018-9480/81/1000-1107$00.75 ©1981 IEEE